

ELECTROPOLISHING OF ADDITIVELY MANUFACTURED HIGH CARBON GRADE 316 STAINLESS STEEL

Pawan Tyagi^{1*}, Tobias Goulet, Christopher Riso, Kate Klein¹, and Francisco Garcia Moreno²

¹Mechanical Engineering, University of the District of Columbia,
4200 Connecticut Avenue NW, Washington, DC, 20008, USA

²Department of Energy's National Security Campus, managed by Honeywell
14520 Botts Road Kansas City, MO 64147, USA

Corresponding author email: ptyagi@udc.edu

ABSTRACT

Improving surface finishing is the critical step in the application of an additively manufactured (AM) component. This paper provides insights into the electropolishing route for the surface improvement of the AM component made up of 316 stainless steel with >6% carbon. We have discussed the Taguchi design of experiment-based process optimization to understand the role of various process parameters. Profilometry and scanning electron microscopy were performed to study the electropolished and unpolished areas of the AM components. Optical profilometry provided an estimate of the amount of material to be removed to achieve shining and smooth AM surface. Optical profilometry also provided analysis of several roughness parameters on the electropolished surface. Electropolishing was effective in reducing the surface roughness below $\sim 0.1 \mu\text{m}$ RMS. This sub μm RMS roughness makes an AM component suitable for major engineering applications. SEM showed distinctively different microstructure on the electropolished surface. We also conducted water contact angle study and spectroscopic reflectance study on electropolished and unpolished AM component surface. Our study revealed that electropolishing is a highly promising route for improving the surface finishing of AM components.

KEY WORDS: Additive manufacturing; electropolishing; surface roughness; stainless steel;

INTRODUCTION:

Additive Manufacturing (AM) can produce nearly ready to use highly complex engineering components. These AM components can be extremely challenging for the conventional subtractive manufacturing route or not possible otherwise. However, to make such AM parts functional it is critical to improve the surface finish of the AM components. An AM part with a rough surface will be vulnerable to premature failure during fatigue loading. It has been observed that increasing surface roughness dramatically reduces the fatigue strength of an engineering component [1, 2]. Similarly, higher surface roughness significantly reduces the high-temperature strength or creep strength [3] of an

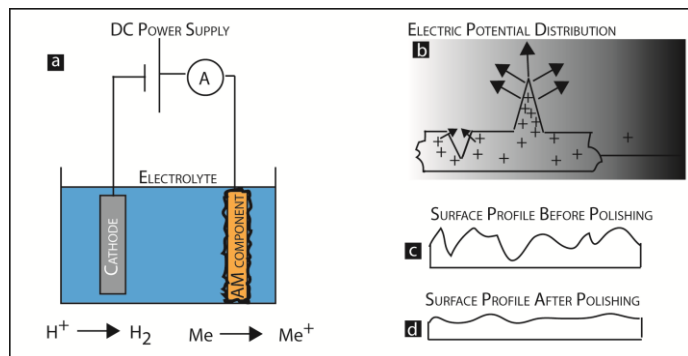


Figure 1: (a) Electropolishing setup facilitate (b) electric field concentration around hills and valley regions on an AM component. (c) A rough surface undergoes faster dissolution around hills and valleys and finally a (d) smoother surface emerges.

engineering component. Higher surface roughness is also found associated with increasing susceptibility to crack generation, and corrosion [4]. Also, integration of AM part with high surface roughness in a complex engineering system with multiple components can create reliability issues. High surface roughness may prevent intimate contact between the component surfaces and hence lead to loose connections [3] and vibration generation. In addition to the surface roughness issue, an AM component may have significantly different surface composition as compared to bulk. Surface finishing is essential to remove the scale from the surface of AM parts to restore the properties of the bulk material on the surface as well.

However, improving surface finish for an AM component can be very challenging based on its intricate design [5, 6]. Popular surface finishing approaches like machining, extrude honing, and sandblasting, may not be applicable for complex AM components [5, 6]. Here we propose the utilization of electropolishing techniques to improve the surface roughness of metal AM components. Electropolishing has a unique advantage because it can reduce surface roughness wherever counter electrode can be placed in the close proximity of target surfaces and electrolyte solution touches the target surface of a metal AM component [5, 6]. Advantageously, an electropolishing solution or electrolyte can easily reach intrusions and hidden surfaces which may be inaccessible by other surface finishing approaches [5]. During electropolishing, the AM component becomes an anode, and a counter electrode is utilized as cathode[7]. The anode and cathode are submerged in an acidic electrolyte, and a current is applied. Electropolishing improves surface finish by removing metal from the surface of a piece, ion by ion [7, 8]. During electropolishing several improvements commences on AM surfaces: (i) electropolishing eliminates surface burrs from delicate and intricate AM components. (ii) electropolishing can effectively improve surface finishing of AM surface by removing scale, oxides, chemicals and surface irregularities, (iii) electropolishing can make a steel surface corrosion resistance by eradicating the surface imperfections that serve as corrosion initiation sites, (iv) electropolishing can significantly improve fatigue life improvement by eliminating micro-cracks and other surface defects on AM parts, (v) electropolishing can ultraclean AM surface. A number of recent studies have applied electropolishing on AM components [9-11]. However, there are is limited study on 316 steel with $> 6\%$ carbon. Such steel has tendency to form cementite like intermetallic phase. This iron carbide phase exhibits different physicochemical properties as compared to other phases present in 316 steel. This 316 steel may be utilized in many critical applications and are likely to benefit from the AM technology. In this study, we have applied electropolishing based surface finishing on 316 steel with high carbon content. The efficacy of the electropolishing is dependent on a number of factors: temperature, agitation, electrolyte composition, and time [7, 12].

Choosing the right combination of electropolishing parameters may be quite challenging [12]. This paper reports our study to optimize the electropolishing process for the 316 high carbon steel AM component. We conducted optical profilometry and scanning electron microscopy (SEM) to quantify the changes surface roughness, and microstructure due to electropolishing. This paper reports our insights about the electropolishing of the steel AM component.

EXPERIMENTAL DETAILS

The surface polishing experiments were conducted on the 316 steel AM samples. These samples were prepared on EOSINT additive manufacturing machine. The 316 stainless steel

metal powder was utilized for this study. The powder particle size was $> 50 \mu\text{m}$. The typical composition of the finished AM components and the powder was 17-19% chromium, 13-15% nickel, 6-8% carbon, 2-3% molybdenum, trace elements, and balance iron. The AM components were produced by direct laser sintering of $\sim 20 \mu\text{m}$ thick layers.

To investigate the utility of the electropolishing approach for reducing surface roughness and improving surface texture we decided to focus on four factors: electropolishing time, temperature, agitation, and electrolyte composition [7, 12]. To limit the number of factors and make our optimization study manageable we fixed the current density around 80 A/dm^2 . However, we separately conducted a number of experiments to evaluate a promising current density for the Taguchi design of experiments. We also referred to numerous prior studies to determine suitable current density for electropolishing on steel AM samples [6, 7, 12-14]. We utilized Qualitek 4 software for the design and analysis. A L9 Taguchi experimental plan [15] was found suitable to accommodate four factors with three levels each (Table 1).

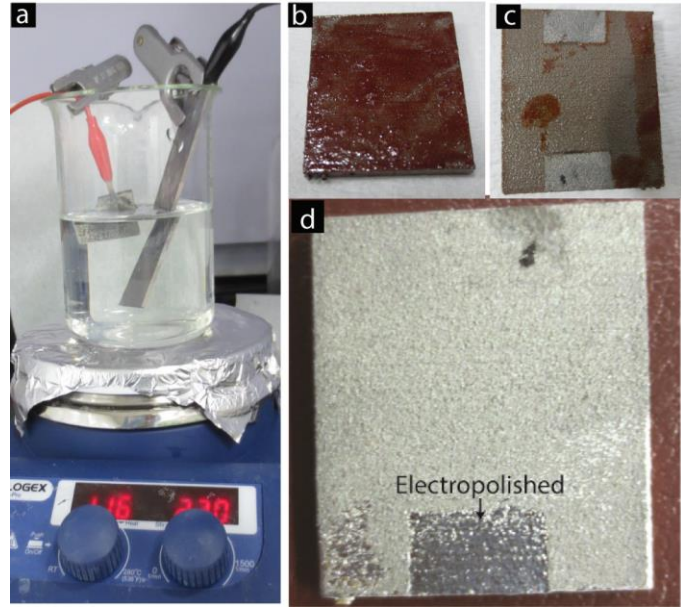


Figure 2: (a) electropolishing setup. (b) photoresist coated AM sample, (c) widows opened in photoresist for electrical contact and electropolishing. (d) An electropolished sample.

Table 1: *L9 Taguchi design of experiment for electropolishing.*

Run#	Time (s)	Temperature (C)	Acid composition	Agitation (rpm)
1	180	82	X	0
2	180	93	Y	200
3	180	104	Z	400
4	240	82	X	400
5	240	93	Y	0
6	240	104	Z	200
7	300	82	Z	200
8	300	93	X	400
9	300	104	Y	0

To conduct the nine Taguchi experiments we utilized a glass beaker with an acidic electrolyte (Fig. 2a). Heating and agitation were performed by using a hot plate with a magnetic stirrer capability (Fig. 2a). In the electrolyte bath, an AM sample and counter electrode were submerged. To ensure that in all the nine experiments we exposed identical surface area we conducted lithography on AM samples. Shipley 1813 photoresist was dip coated on AM samples in a class 1000 clean room environment (Fig. 2b). Subsequently, the photoresist coated samples were heated on the hot plate at 100 °C for 20 minutes. Prolonged baking at high temperature was accomplished to make photoresist sufficiently hard so that it can withstand acid solution and other experimental conditions (Fig. 2a). Successively, we opened a $\sim 0.5 \text{ cm}^2$ window in the photoresist shield by selective chemical dissolution of photoresist (Fig. 2c). All the prepared samples were subjected to electropolishing as per the L9 experimental plan (Table-1). In the Table-1 X, Y and Z denoted three acid bath composition we utilized. We produced 100 mL electrolyte solution in water by adding 85% phosphoric acid and 98% sulfuric acid [7, 16]. Other than water, solution X contained 41 g phosphoric acid and 45 g sulfuric acid, solution Y contained 49 g phosphoric acid and 41 g sulfuric acid, and solution Z contained 15 g phosphoric acid and 63 g sulfuric acid. The selection of the electrochemical bath composition was based on prior literature [5, 6, 12, 13, 16]. After each experiment photoresist was removed from each AM sample and roughness measurements were performed on the electropolished and unpolished areas to determine the efficacy of each experiment. For the roughness measurement, the PCE RT 1200 surface profilometer was utilized. Periodically, the roughness meter was calibrated with the known standard sample. For this study we performed linear scan of 5 mm length. This may be one of the reason for relatively higher Ra values observed in Taguchi design of experiment.

After conducting the design of the experiment, we also conducted electropolishing on the cylindrical AM component. The lower part of the cylinder was submerged in the electrolyte bath and was subjected to electropolishing. The top part was protected by applying the photoresist insulation coating on the sample surface. After the electropolishing step, the photoresist coating was removed by submerging the whole sample in the Shipley 1165 photoresist remover. The optical profilometry was performed with Zeta 20 and Filmetrics optical profilometers to compare the change in roughness due to electropolishing. We also performed scanning electron microscopy to study the difference in elemental composition and microstructure before and after electropolishing.

We have also attempted electropolishing with the optimized parameters on AM steel samples with internal surfaces. However, only those samples for which we designed the 3D model to allow the access of a counter electrode in the proximity of target internal surface of AM component, yielded satisfactory results.

RESULTS AND DISCUSSION:

Initially we conducted electropolishing on the rectangular shaped AM component. A 0.5 cm^2 area was opened in the photoresist protection to enable the electropolishing in the controlled area of AM components. We conducted roughness measurements on unpolished and electropolished areas on these rectangular shaped AM sample. The roughness measurements on the unpolished area are equivalent to roughness before the electropolishing. Table 2 summarizes the quantitative roughness measurements on the AM components. For Taguchi analysis we utilized the difference in average roughness for each sample to avoid any error caused by the difference of the starting

surface roughness for different samples. For Taguchi analysis we applied “bigger is better” roughness difference criteria. Invariably, after electropolishing the roughness of each sample reduced.

Table 2: *Roughness measurement on nine samples before and after electropolishing. The last column shows the difference of sample roughness before and after electropolishing.*

Run#	Before (μm)	After (μm)	Avg. difference in roughness (μm)
1	6.035 ± 0.103	4.653 ± 0.203	$y_1 = 1.382$
2	8.768 ± 0.213	4.790 ± 0.111	$y_2 = 3.978$
3	4.911 ± 0.082	3.903 ± 0.050	$y_3 = 1.008$
4	5.388 ± 0.026	4.941 ± 0.269	$y_4 = 0.447$
5	4.639 ± 0.054	2.835 ± 0.067	$y_5 = 1.804$
6	7.389 ± 0.106	1.996 ± 0.126	$y_6 = 5.393$
7	5.201 ± 0.090	3.586 ± 0.236	$y_7 = 1.615$
8	7.440 ± 0.078	4.306 ± 0.314	$y_8 = 3.134$
9	7.695 ± 0.128	3.871 ± 0.063	$y_9 = 3.824$

Using the experimental data for each run (Table 2) the data analysis was performed. Initially, we computed the effect of different levels of four parameters (Fig. 3). We calculated the level total and their averages. To accomplish this objective, results of all trials involving the particular level of parameters are added, and then divided by the number of data points added. For instance, for the three levels of time parameter, the following equations were adopted [17].

$$A1 = \text{Time}(180 \text{ sec}) = y_1 + y_2 + y_3 \quad (1)$$

$$A2 = \text{Time}(240 \text{ sec}) = y_4 + y_5 + y_6 \quad (2)$$

$$A3 = \text{Time}(300 \text{ sec}) = y_7 + y_8 + y_9 \quad (3)$$

Subsequently, the averages $\bar{A}(1)$, $\bar{A}(2)$, and $\bar{A}(3)$ were calculated by dividing A(1), A(2), and A(3) by three, since each level of time parameter appeared in the three trials (Table 2). Likewise, average values of each level of all the parameters were calculated.

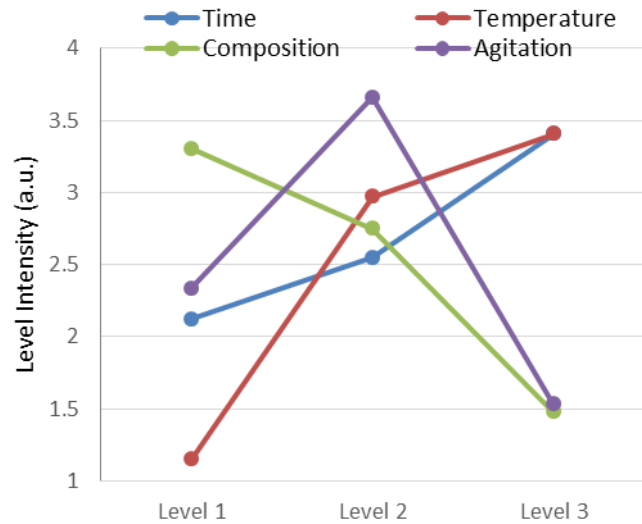


Figure 3: Effect of three levels of each factor.

The average values of each level of all the parameters were plotted to provide the insight about their relative impact (Fig. 3). The electropolishing performance kept increasing with temperature (Fig. 3). However, we are unsure if this trend will continue if one further increases the temperature. It is expected that secondary processes may interfere. Interestingly, medium level agitation was found to yield better electropolishing. It is quite likely that higher agitation may affect the fluid dynamics near AM surface and result in turbulence. The turbulent fluid flow may interfere with the electrolyte's electropolishing process. However, medium level agitation is expected to be good enough to drive away the electropolishing residue from the AM sample surface (Fig. 3). Taguchi analysis provided clear insight about the electrolyte bath composition. According to our analysis composition X, which contained 41 g phosphoric acid and 45 g sulfuric acid, produced the highest quality electropolishing. Electropolishing appears to get better with time. We anticipate that prolonged electropolishing can gradually reduce the roughness significantly.

It is noteworthy that Taguchi analysis is also capable of determining the degree of interaction among factors [15]. We made six pairs (4C_2) by selecting two variables at a time using the permutation-combination rule. Taguchi analysis ranked the degree of interaction in terms of % interaction severity index [15]. We found that time and electrolyte bath composition were strongly correlated (Fig. 4). This result can be explained by noting that electrolyte bath composition affects the electropolishing rate. Hence, the amount of electropolishing

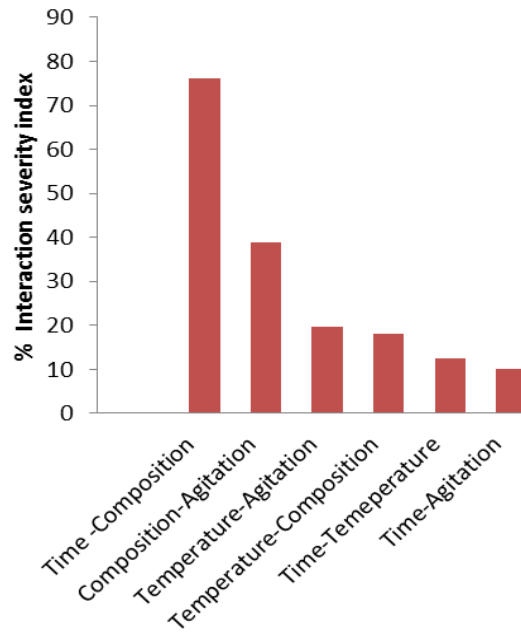


Figure 4: Interaction severity index between two factors.

accomplished in a given time period is dependent on electrolyte bath composition. We also noted that agitation and electrolyte bath composition were also correlated (Fig. 4). It seems that efficacy of one electrolyte composition is strongly related to the agitation. Other factors were also found to be correlated with another. However, time and agitation were the least correlated (Fig. 4)

To calculate the relative impact of the four parameters, we performed Analysis of variance (ANOVA) [15]. We calculated the sum of all the results and denoted it by T . The magnitude of T was found to be 22.525. Subsequently, a correction factor ($C.F.$) was calculated by dividing the square of sum by the total number of experiments ($C.F. = T^2/9$). We computed the sum of squares (S) by using the following equation: $S = T^2 - C.F.$ To proceed to the next step sum of squares due to a parameter were calculated. For instance the sum of squares for the parameter time (A) were calculated using equation (4).

$$SS_A = [A(1)^2/3 + A(2)^2/3 + A(3)^2/3] - C.F. \quad (4)$$

Similarly, the sum of squares for three other parameters temperature (B), composition (C), and agitation (D) was computed. In the next step error sum of squares (SS_e) was calculated by utilizing the equation (5).

$$SS_e = SS_T - (SS_A + SS_B + SS_C + SS_D) \quad (5)$$

The degree of freedom for all the parameters was calculated. The total degree of freedom was eight; for each parameter degree of freedom was two (number of levels-1). Subsequently, the mean square of variance was calculated for different parameters by dividing the sum of squares with the degree of freedom for the individual parameters. The mean square of variance for the error was calculated by dividing the SS_e with a degree of freedom for the error. Next, we computed the pure sum of square by following the following equation (6)

$$SS'_A = SS_A - (V_e \cdot F_A) \quad (6)$$

Similarly, pure sums were calculated for other parameters too (Table 3). Finally contribution (P) for the individual parameters was calculated by utilizing the following equation.

$$P_A = SS'_A / SS_T \quad (7)$$

Similarly, the impacts of the other three parameters were computed and tabulated in Table 3.

Table 3: ANOVA analysis of four parameters. The last column of the table shows the impact of individual parameter.

Factors	DOF(f)	Sum of Squares	Variance (V)	Pure Sum()	P
Time	2	0.817	0.408	0.817	0.038
Temperature	2	8.626	4.313	8.626	0.398
Composition	2	5.268	2.634	5.268	0.243
Agitation	2	6.954	3.477	6.954	0.321

The P values for the individual can be converted into percentage by multiplying by 100. Taguchi analysis suggested that temperature was the most influential parameter for electropolishing. The temperature parameter accounted for a contribution of ~40%. The agitation and electrochemical bath composition were at the second and third place, respectively (Table 3). The electropolishing period was found to be least influential. In the case of electrochemistry oxidation and reduction, processes are generally exponentially dependent on temperature [7, 13].

Table 4: *Elemental analysis in the unpolished and electropolished area.*

<i>Element</i>	<i>Unpolished (%)</i>	<i>Electropolished (%)</i>
Iron	23.2±0.1	59.7±0.0
Chromium		15.1±0.1
Oxygen	54.4±0.3	6.3±1.3
Nickel		8.2±0.6
Carbon	10.5±0.4	6.9±0.9
Silicon		1.0±0.6
Nitrogen		2.8±2.0
Sulfur	11.9±0.1	

Hence, the temperature being most influential is justifiable. In the case of electropolishing, agitation is also critically important to ensure the smooth material removal after surface etching of AM components. We observed that without agitation yellow residue agglomerated adjacent to the sample surface. Agitation helped disperse this residue and ensure that electrolyte properties do not vary drastically during electropolishing. For electropolishing, the electrolyte bath also played a significant role and had a 24.32% contribution in determining electropolishing quality. Finally, time was also found to affect surface roughness.

Subsequently, we utilized Taguchi analysis to yield optimum combination of levels for four parameters to yield the optimum electropolishing effect. According to the Taguchi analysis time 300 seconds, temperature 105 °C, composition X, and agitation at 200 rpm is projected to yield the highest difference in the roughness before and after

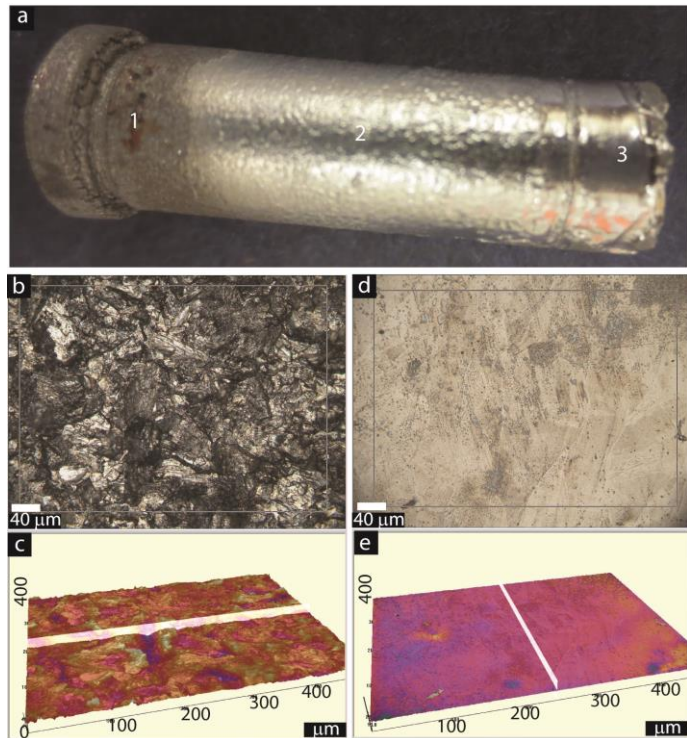


Figure 5: Electropolishing of a cylindrical AM component: (a) Cylindrical AM component showing unpolished (1), and electropolished (2, 3) sections. (b) Optical microscope image of the top side and the (c) 3D perspective image in the unpolished area. Optical microscope image of the (d) top side and the (e) and 3D perspective image from the electropolished area.

electropolishing. This optimum combination of levels for four factors was estimated to give 5.7 μm Ra roughness difference. To cross check this estimation we conducted electropolishing with the optimized parameters and found that difference in roughness was 4.25 μm (Fig. 2d). We hypothesize that the small difference between experimentally observed roughness differences as compared to the predicted one is due to potential variability in the experimental conditions. Specifically, it may be due to leakage of current through the photoresist insulator, and counter electrode surface condition, etc.

After determining the suitable combination of electropolishing parameters, we attempted surface roughness reduction on cylindrically shaped samples. We hypothesized that longer duration would gradually flatten out high and low sections on the surface of as produced AM samples. Hence, prolonged electropolishing is expected to yield highly smooth morphology. Hence cylindrical AM samples were electropolished for ~10 minutes.

We observed that a stainless steel cylindrical sample could be electropolished to yield very smooth surface roughness. In this study, we are specifically discussing a sample that was subjected to electropolishing treatment for different periods along its length. The unpolished section is designated as zone 1, the area with medium electropolishing is designated as the zone 2, and the lowermost section with maximum electropolishing is designated as zone 3 (Fig. 5a). The prolonged electropolishing with the optimized parameters produced a very smooth surface (Fig. 5a). The quantitative roughness measurements were performed with Zeta 20 optical profilometer. Optical images of the zone 3 (smoothest electropolished area) and Zone 1 (unpolished rough area) are shown in Fig. 5b and Fig. 5c. The roughness measurement was performed in the $\sim 495 \mu\text{m} \times 372 \mu\text{m}$ area.

The smoothest electropolished area showed $\sim 0.091 \mu\text{m}$ Ra (Fig. 5d-e) and unelectropolished area exhibited $\sim 1.88 \mu\text{m}$ Ra. However, it must be noted that roughness measurement over a broad area of the electropolished section includes many porosities. The $495 \mu\text{m}$ long line scan on the electropolished surface in the smoothest region yielded a roughness of $0.07 \mu\text{m}$ Ra. This result signifies that electropolishing is capable of achieving the even smoother surface finish.

We also investigated the amount of material removal necessary to achieve the highly smooth surface finish. To estimate the required material removal we determined the difference in height for the electropolished and unpolished area. The depth profiling was accomplished by measuring the sample height along a scan

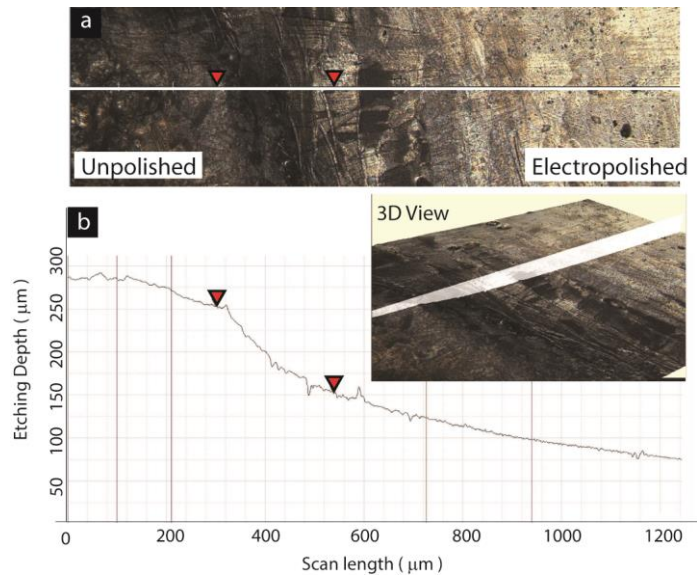


Figure. 6. Thickness difference between unpolished and electropolished area. (a) Optical microscope image showing the white color line along which thickness measurement was performed. (b) Etching depth vs. distance profile along the white color scan line on image (a). The inset of (b) shows the difference in height with respect to unpolished section plane.

traversing from unpolished to the electropolished area (Fig. 6a). The two red color arrows mark the area where the sharp change in height was determined. The typical difference was around $\sim 200 \mu\text{m}$ (Fig 7b). This result is critically important in determining the tolerance required to accommodate electropolishing as the post-processing step. The inset figure shows a cross section along the scan direction. The back side of 3D view is kept at the unpolished surface height. The white area in 3D view shows that as one moved from unpolished to polished area, material removal occurred (Fig. 6b).

We have also electropolished the samples with internal volumes. The internal surface was not affected by the electropolishing on the AM samples where a counter electrode could not be placed in the proximity of the internal surfaces. However, outer surface area exhibited remarkable improvement in the surface finishing due to electropolishing. For the quantitative analysis, we determined the maximum peak height (S_p), maximum valley depth (S_v), maximum height difference between peak and valley (S_z), arithmetic mean height (S_a), and root mean square (RMS) of height (S_q). The surface skewness factor (S_{sk}) and surface kurtosis (S_{ku}) were also determined. We recorded these roughness parameters in $0.2 \times 0.17 \text{ mm}^2$ area on eight different locations. The magnitude (S_p) was $166.35 \pm 18.65 \mu\text{m}$ for the unpolished AM surface which was reduced to $16.38 \pm 6.65 \mu\text{m}$ for the electropolished AM samples. Similarly, the depth of valley (S_v) was $60.12 \pm 20.10 \mu\text{m}$ for the AM surface before electropolishing. After electropolishing S_v reduced to $28.12 \pm 8.31 \mu\text{m}$. The difference between the height of the tallest peak and deepest valley (S_z) for the AM sample before electropolishing was $226.44 \pm 17.67 \mu\text{m}$. After electropolishing S_z reduced to $44.50 \pm 13.45 \mu\text{m}$. The surface roughness parameter (S_a) for the unpolished surface was $13.88 \pm 2.65 \mu\text{m}$. After electropolishing S_a reduced to $3.0 \pm 0.75 \mu\text{m}$. The RMS roughness (S_q) for the unpolished AM surface was determined to be $17.37 \pm 3.02 \mu\text{m}$. After electropolishing S_q decreased to $3.77 \pm 0.85 \mu\text{m}$. The surface skewness factor (S_{sk}) magnitude was 0.10 ± 0.98 for the unpolished surface, which indicates that the number of hills and valleys are almost in the same proportion to one another. However, S_{sk} parameter became negative for the electropolished samples indicating the dominance of cavities. S_{sk} was -0.29 ± 0.85 for the electropolished sample. The surface kurtosis (S_{ku}) describes the peakedness of the surface topography. If $S_{ku}=3$, then the distribution is ideal Gaussian-like. S_{ku} was calculated for the whole area and determined to be 2.2 for the unpolished AM sample and 3.4 for the electropolished. This data indicates that a electropolished sample was significantly biased towards having a higher proportional number of valleys. We also found that electropolishing can be performed on the internal volume of the AM steel components by considering the counter

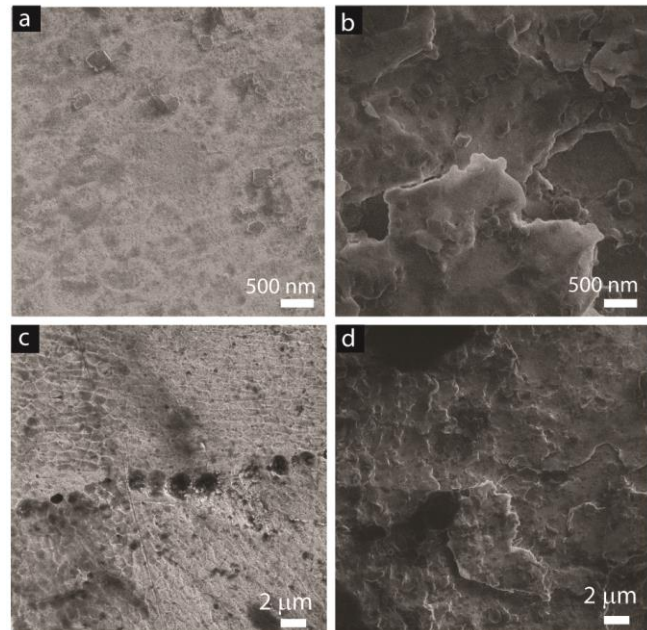


Figure. 7. SEM images from the zone 1 and zone 3. (a, c) Images from electropolished area at various magnification. (b and d). Images from the unpolished area at various magnifications.

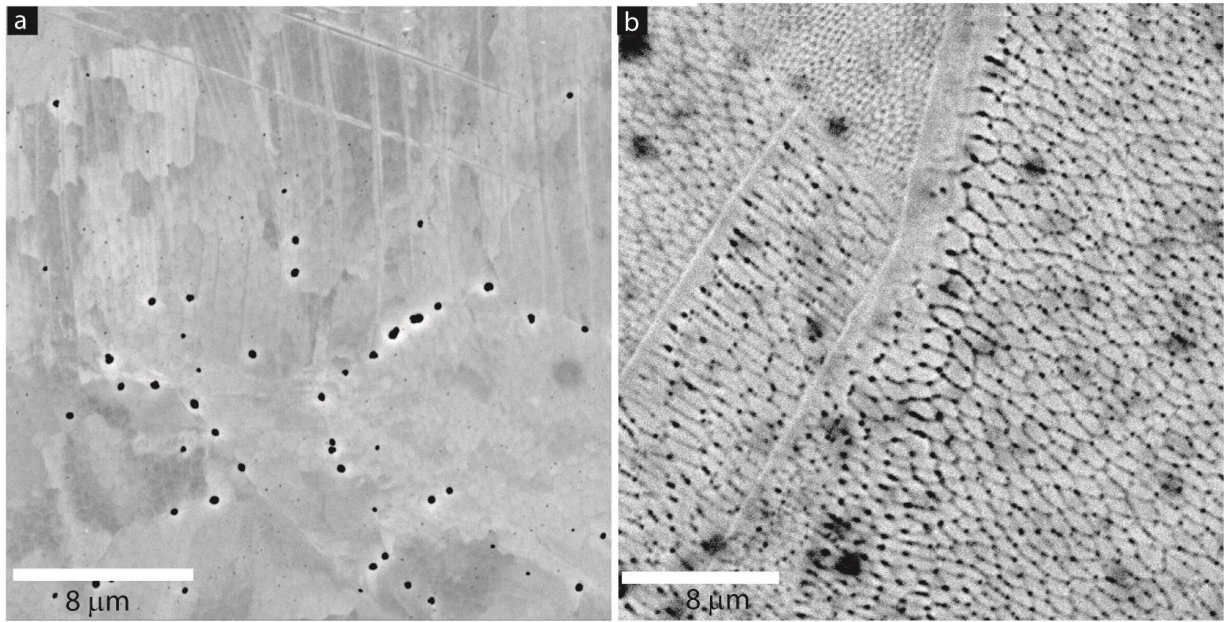


Figure. 8. SEM images obtained using backscattering detector from (a) optimally electropolished 316 AM sample and (b) from excessively electropolished AM sample.

electrode access during the design stage. We prepared cubic AM samples with ~1 cm diameter holes to allow counter electrode to easily enter into the internal volume. Electropolishing effectively reduced the surface roughness of the internal volume. Hence, one can design an AM component by considering the needs of electropolishing in mind.

We also performed scanning electron microscopy (SEM) to investigate the difference in composition and microstructure of the electropolished and unpolished area. The Electron Dispersive Spectra (EDS) study showed that surface composition was entirely different and contained high oxygen content. Interestingly, after the removal of ~ 200 μm, thick material from the surface during electropolishing yielded typical stainless steel composition. The composition of the electropolished area was akin to the composition of stainless powder utilized for the AM. It is noteworthy the unpolished surface (Fig.7a) was gray in color and signified the change in composition. The typical steel surface is shiny and has silver color as shown in the electropolished area (Fig. 5). This result is of critical importance when welding of the AM component of other parts is important. Also, physio-chemical properties of the unpolished surface will be entirely different as compared to the stainless steel surface.

The microstructure of the electropolished and unpolished surface was expected to be quite different. We performed SEM study and found that at high magnification the electropolished surface was predominantly featureless (Fig. 7a), as compared to the unpolished area (Fig. 7b). The unpolished section on the AM produced cylinder contained the flaky pattern. At medium magnification, the electropolished surface appeared featureless. However, setting the SEM parameters to yield higher contrast revealed various microstructural features (Fig. 7c). On the other hand the unpolished section at the same magnification still, exhibited a flaky pattern (Fig. 7d).

We also utilized back scattering detector of the SEM to study the electropolished AM samples. We found that an optimally electropolished 316 AM sample yielded quite regular microstructure

with numerous pits or cavities. Overall surface is quite smooth and exhibited $\sim 0.5 \mu\text{m}$ roughness (Fig. 8a). It is noteworthy that Fig.8a also contain sub-micron grains which are faintly observable in Fig.8a. However, Fig.7d provide a better contrast. We became interested in investigating if we could etch away the pits or cavities seen in the Fig.7d and Fig.8a. For that we conducted electropolishing for the extended period and studied the 316 AM steel sample with the back scattering detector of the SEM. The microstructure of the excessively electropolished AM sample turned out to be significantly different (Fig. 8b). As seen in the SEM image the several pits area started to disappear, but several continued to persist (Fig.8b). This study suggest that pits or cavities observed after electropolishing possessed different depth. Interestingly, excessively electropolished sample showed very clear presense of near hexagonal grains (Fig.8b). The small hexagonal grains contain rather smooth or flat interior regions but the grain boundary region is significantly etched. It appears that grain boundary region is more susceptible to etching as compared to interior region of the grains. We surmise that at the grain boundary cementite phase was expected to be present for the high carbon 316 steel grade as used in this study. Presumably, the cementite along the grain boundaries etched away faster than the low carbon phase present within the interior of the grain.

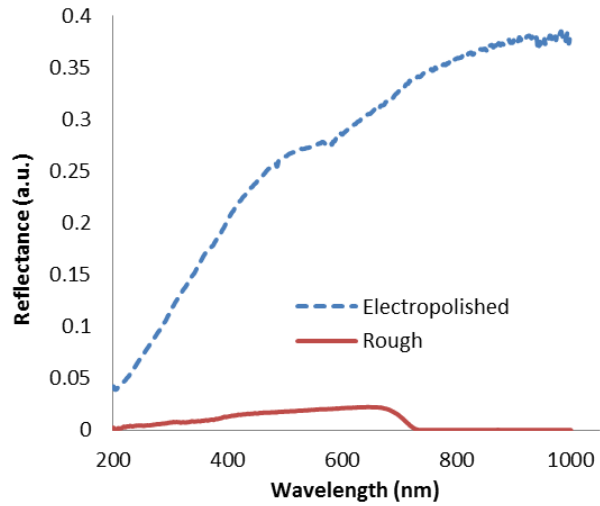


Figure 9: Reflectance characteristics of the electropolished and unpolished (rough) surface of an AM steel component.

We performed spectroscopic reflectance to further determine the properties of the top surface of an AM component before and after electropolishing. We utilized Semiconsoft M-Probe (M probe reflectivity meter) for this study. The reflectance from the as produced AM component surface was significantly less than that from the electropolished areas. Moreover, the bare AM sample also was unable to absorb radiation beyond 730 nm wavelength (Fig. 8). This result indicates that AM surface may absorb radiation, however, electropolished AM component reflect the radiation back. This property is of critical importance where AM component is expected to be radiation sensitive. It is noteworthy that amount of radiation absorbed can vary the temperature of the AM component and hence design engineers should be cognizant about characteristics of various surface finishing.

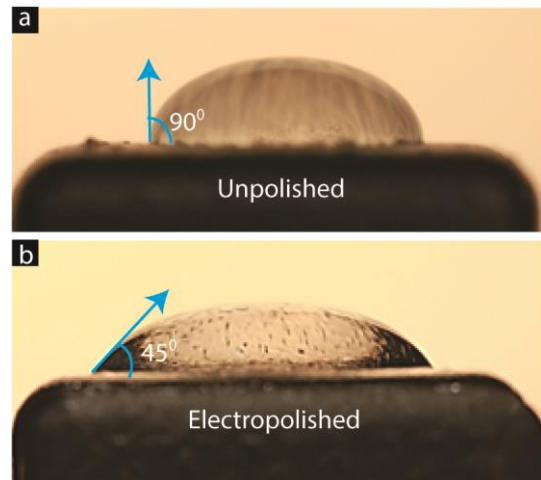


Figure 10: Water contact angle measurement on (a) unpolished and (b) electropolished AM steel component.

We also studied the difference in the surface chemistry of the unpolished and electropolished AM samples. For the study of surface chemical properties, we utilized water contact angle measurement. In this experiment ~100 μL water drop was introduced on cleaned and dried AM sample surfaces. The unpolished 316 AM steel sample formed $\sim 90^\circ$ angle at the junction of water, AM surface, and air (Fig. 10a). However, the electropolished AM sample yielded $\sim 45^\circ$ contact angle. The smaller contact angle indicates that the electropolished sample became significantly hydrophilic, as compared to the unpolished AM sample. Further study by XPS like sensitive surface measurement may provide more profound insights about the surface chemistry of electropolished samples.

CONCLUSIONS

In this paper, we demonstrated the utilization of the electropolishing approach to improving the surface finish of as produced 316 high carbon stainless steel metal additive manufacturing components. To systematically understand the impact of electropolishing factors such as temperature, agitation, electrolyte bath composition, and time we have employed the Taguchi design of experiment approach. We conducted parameter optimization on the rectangular samples. The results of Taguchi design of experiments were implemented on cylindrical shaped AM samples. Electropolishing with optimized parameters could drastically improve the surface finish of the AM components. The typical surface roughness decreased below $\sim 0.1 \mu\text{m Ra}$. Electropolishing also removed the scale from the AM component surface and brought out the surface with typical stainless-steel composition and bright luster. The electropolished surface possessed a significantly smaller defect population on the AM surface. We also found that nearly $\sim 250 \mu\text{m}$ thick material should be removed during electropolishing to attain highly smooth surface finish. Scanning electron microscope imaging revealed that as produced AM steel component had flaky morphology, along with pits like features. The microstructure of the electropolished surface was dramatically better than that of as produced AM surface. Electropolishing was effective in improving surface finishing of AM component if a counter electrode could be placed in the close proximity of the AM component.

ACKNOWLEDGMENTS

We gratefully acknowledge the funding support from the Department of Energy-National Nuclear Security Agency (Subaward No. 0007701-1000043016). This work is in part supported by the Department of Energy's Kansas City National Security Campus. The Department of Energy's Kansas City National Security Campus is operated and managed by Honeywell Federal Manufacturing & Technologies, LLC under contract number DE-NA0002839. We also thank Sebastian and Matt Jobins of Nanoscience Instrument for the assistance with SEM imaging. We appreciate assistance from Jim Elmen of Filmetrics for optical profilometry.

REFERENCES

- [1] H. Sasahara, "The effect on fatigue life of residual stress and surface hardness resulting from different cutting conditions of 0.45% C steel," *International Journal of Machine Tools and Manufacture*, vol. 45, pp. 131-136, 2005.
- [2] M. Suraratchai, J. Limido, C. Mabru, and R. Chieragatti, "Modelling the influence of machined surface roughness on the fatigue life of aluminium alloy," *International Journal of fatigue*, vol. 30, pp. 2119-2126, 2008.
- [3] M. Ranjbar-Far, J. Absi, G. Mariaux, and F. Dubois, "Simulation of the effect of material properties and interface roughness on the stress distribution in thermal barrier coatings using finite element method," *Materials & Design*, vol. 31, pp. 772-781, 2010.

- [4] G. Burstein and P. Pistorius, "Surface roughness and the metastable pitting of stainless steel in chloride solutions," *Corrosion*, vol. 51, pp. 380-385, 1995.
- [5] H. Zhao, J. Van Humbeeck, J. Sohler, and I. De Scheerder, "Electrochemical polishing of 316L stainless steel slotted tube coronary stents," *Journal of Materials Science-Materials in Medicine*, vol. 13, pp. 911-916, Oct 2002.
- [6] F. Nazneen, P. Galvin, D. W. M. Arrigan, M. Thompson, P. Benvenuto, and G. Herzog, "Electropolishing of medical-grade stainless steel in preparation for surface nano-texturing," *Journal of Solid State Electrochemistry*, vol. 16, pp. 1389-1397, Apr 2012.
- [7] D. Landolt, "Fundamental-aspects of electropolishing," *Electrochimica Acta*, vol. 32, pp. 1-11, Jan 1987.
- [8] T. Hryniewicz, K. Rokosz, and R. Rokicki, "Electrochemical and XPS studies of AISI 316L stainless steel after electropolishing in a magnetic field," *Corrosion Science*, vol. 50, pp. 2676-2681, Sep 2008.
- [9] S. Habibzadeh, L. Li, D. Shum-Tim, E. C. Davis, and S. Omanovic, "Electrochemical polishing as a 316L stainless steel surface treatment method: Towards the improvement of biocompatibility," *Corrosion Science*, vol. 87, pp. 89-100, Oct 2014.
- [10] V. Urlea and V. Brailovski, "Electropolishing and electropolishing-related allowances for IN625 alloy components fabricated by laser powder-bed fusion," *International Journal of Advanced Manufacturing Technology*, vol. 92, pp. 4487-4499, Oct 2017.
- [11] C. Rotty, M. L. Doche, A. Mandroyan, and J. Y. Hihn, "Electropolishing Behavior of Additive Layer Manufacturing 316L Stainless Steel in Deep Eutectic Solvents," in *Selected Proceedings from the 231st Ecs Meeting*. vol. 77, M. Manivannan, S. Narayan, R. Kosteki, C. Johnson, and P. B. Atanassov, Eds., ed Pennington: Electrochemical Soc Inc, 2017, pp. 1199-1207.
- [12] C.-C. Lin and C.-C. Hu, "Electropolishing of 304 stainless steel: Surface roughness control using experimental design strategies and a summarized electropolishing model," *Electrochimica Acta*, vol. 53, pp. 3356-3363, Mar 10 2008.
- [13] C.-C. Lin, C.-C. Hu, and T.-C. Lee, "Electropolishing of 304 stainless steel: Interactive effects of glycerol content, bath temperature, and current density on surface roughness and morphology," *Surface & Coatings Technology*, vol. 204, pp. 448-454, Nov 15 2009.
- [14] S. Magaino, M. Matlosz, and D. Landolt, "An impedance study of stainless-steel electropolishing," *Journal of the Electrochemical Society*, vol. 140, pp. 1365-1373, May 1993.
- [15] G. Taguchi, *Introduction to quality engineering: designing quality into products and processes*, 1986.
- [16] S. C. Chen, G. C. Tu, and C. A. Huang, "The electrochemical polishing behavior of porous austenitic stainless steel (AISI 316L) in phosphoric-sulfuric mixed acids," *Surface & Coatings Technology*, vol. 200, pp. 2065-2071, Dec 2005.
- [17] S. Kumar, P. Kumar, and H. S. Shan, "Optimization of tensile properties of evaporative pattern casting process through Taguchi's method," *Journal of Materials Processing Technology*, vol. 204, pp. 59-69, Aug 2008.